



2019 Department of Defense – Allied Nations Technical Corrosion Conference



Paper No. 2019-0218_0314_000077

THE DEVELOPMENT OF A METHOD FOR COMPLEX ENVIRONMENT CORROSION FATIGUE TESTING

Sarah E. Galyon Dorman, SAFE Inc

Jason H. Niebuhr, SAFE Inc

Jenifer S. Locke, The Ohio State University

Brandon Free, The Ohio State University

Keywords: Atmospheric Corrosion, Fatigue, ozone, temperature, 7085

ABSTRACT

The objective of this project is to investigate and determine the individual and combined effects of atmospheric exposure as a function of relative humidity (RH), temperature (T), surface salt contamination, and ozone on corrosion fatigue (CF), in a modern and legacy 7xxx series aerospace aluminum alloys (AA7085-T7451 and 7075-T651) as a means of providing enhanced knowledge that can improve service life predictions and maintenance for Department of Defense aircraft. To accomplish this objective, CF crack growth kinetics (da/dN) will be quantified as a function of independently controlled individual atmospheric exposure parameters to understand the individual effect of each parameter on CF. Secondly, CF da/dN will be quantified as a function of complex combinations of atmospheric exposure parameters utilizing a modular system for complex environmental and mechanical testing. This combined testing program will allow for a better understanding of what environmental parameters are most critical for developing an accelerated laboratory atmospheric corrosion fatigue protocol relevant for aerospace aluminum applications. A secondary goal of this program is to begin to determine how reproducible atmospheric corrosion fatigue data is between laboratories.

INTRODUCTION

Age-hardenable aluminum alloys are used for many aerospace applications, where high strength and low density are required. In service, these alloys must withstand both demanding mechanical loads and corrosive environmental conditions. For components made of these alloys, problems may occur when mechanical stresses are present with a corrosive environment. In fact, several reviews of aircraft structural failures and teardown inspections have concluded that fatigue, mechanical degradation involving cyclic stresses which can cause material failure at stress levels significantly lower than the tensile yield stress, and corrosion dominate aerospace component failures [1,2]. Additionally, 78% of corrosion damage sites identified during teardown were found to have initiated fatigue cracks [2]. These findings demonstrate the importance of quantifying and understanding the synergistic effects of corrosion and mechanical stresses, a phenomenon referred to as environment assisted cracking (EAC).

EAC is a material degradation process that occurs because of the deleterious interaction of mechanical stresses and an external corrosive environment that uniquely localizes within an occluded crack. When cyclic fatigue loads are encountered, EAC is termed corrosion fatigue (CF). The precise mechanism by which EAC occurs in aero-

space aluminum alloys is still debated, but it is likely either hydrogen environment assisted cracking (HEAC aka hydrogen environment embrittlement, HEE) or film rupture - anodic dissolution or some combination of these two [3,4,5,6]. Although the mechanism is still debated, two things are generally accepted: (1) the chemical and electrochemical conditions of the bulk environment are not maintained down the crack, particularly at the tip, and (2) it is the stress state and chemical/electrochemical conditions local to the crack tip that control EAC. As the Department of Defense (DoD) extends the service life of their aircraft or acquires new aircraft, understanding combined atmospheric environmental mechanical effects is paramount.

The wide breadth of knowledge, characterization, and prior research on CF performance of aerospace aluminum alloys has focused on full immersion in aqueous solutions, laboratory-moist air or pure water vapor [7-34]. Yet aircraft operate not only under a spectrum of mechanical loading, but also a spectrum of environmental conditions [35]. Temperature, humidity, atmospheric gas composition, chloride concentrations, and light exposure all vary as a complex function of geographical location, seasonal weather patterns, diurnal cycle, flight segments, and mission profile mix. Atmospheric exposure involves gas and particle pollutants dissolved in water vapor, rain, snow, fog, aerosol particulates and other debris. Although not inclusive, these pollutants include oxides of nitrogen (NO, NO₂, etc.), sulfur dioxide (SO₂), nitrous oxide (N₂O₂), nitric acid (HNO₃), hydrogen chloride (HCl), hydrogen peroxide (H₂O₂), chlorine atoms (Cl), ozone (O₃), ammonia (NH₃), chlorine nitrate (ClONO₂), and hydroxyl (OH) [36,37]. Such contaminants collect on a metal surface and absorb moisture to deliquesce an electrolyte layer, or more likely electrolyte droplets, at partial pressure (P_{H₂O}) lower than expected for pure water condensation on a clean surface. Additionally, the chemical/electrochemical conditions local to the crack tip, which control CF, are likely to be very different under atmospheric conditions as diffusion, ion migration, and convective mixing with a bulk solution cannot occur.

Corrosion related research has resulted in noteworthy advances in understanding the kinetics of atmospheric corrosion. Current test methodologies, such as neutral salt fog described in ASTM¹ B117, often correlate poorly with field exposure [38, 39, 40]. The addition of ozone, UV light, and control of relative humidity was shown to create corrosion in highly pure silver (Ag) samples similar to outdoor exposures due to the formation of reactive oxidizing species [39,40]. Carbon steel and Al-Mg alloys samples demonstrated similar discrepancies between lab testing and actual field exposures that were mitigated with the addition of ozone and UV light [41]. Chlorides in conjunction with strong oxidizers like ozone react to create species that attack the substrate material. Furthermore, the aerosols that deposit chlorides on field exposure samples can vary in size, composition and acidity [42]. These variations have proven in recent experiments to influence corrosion morphologies and rates [41].

Due to limited prior research on EAC in atmospheric environments that create surface electrolyte droplets or continuous/semi-continuous layers, little is known about the ability to translate the well quantified full immersion EAC properties and behavior of many material systems to atmospheric service environments. Additionally, as most material qualification testing for aircraft alloys occurs in laboratory air or full immersion in aqueous sodium chloride, there is a concern that the fatigue crack growth rates being used are either too aggressive or too conservative leading to incorrect damage estimates and inspection intervals. When considering aerospace atmospheric influences on CF, investigations have focused on a more limited set of parameters. Likewise it may also suggest that the most critical time for environmental exposure on aircraft may not be on the ground, but rather during ascent and descent when mechanical loading is occurring in conjunction with a wetting/drying cycle due to change in altitude. This research aims to understand how individual environmental atmospheric corrosion parameters effect fatigue crack growth, specifically ozone, temperature, salt film, UV-light and relative humidity as well as how those combined environmental parameters change fatigue crack growth. This results will allow for determination to be made on the critical environmental inputs required to produce a consistent, relevant accelerated atmospheric corrosion fatigue methodology to allow for better aircraft life predictions. A secondary aim of this project to understand how much variability occurs when different laboratories complete corrosion fatigue testing using the same complex environmental and mechanical loading parameters.

EXPERIMENTAL PROCEDURE

The specimen selected for this work was the eccentrically loading single edge notch tension (ESE(T)) sample. This sample design was selected because the sample is an ASTM E647 approved sample geometry and requires limited material, while having a single crack front. The crack growth rate for the samples was measured using Fracture

¹ ASTM International 100 Barr Harbor Drive West Conshohocken, PA 19428

Technology Associates (FTA)² direct current potential drop (dcPD) software with either a 50 MPa or 100 MPa MTS³ servohydraulic test frame. All samples were made of a legacy, aluminum-zinc-magnesium-copper alloy (Al-Zn-Mg-Cu) (AA) 7075-T651 or a modern alloy 7085-T7451 with the rolling direction in line with the specimen length. Figure 1 shows the sample design. Figure 2 shows the results of the constant ΔK , R testing in both laboratory air and 0.06 M sodium chloride (NaCl) full immersion solution for AA7075-T651 samples. It should also be noted that the crack growth rate appears to slightly increase over time for the middle data set in Figure 2. This error is due to posttest correction using the final crack length measured with an optical microscope according to ASTM E647 [43]. For a constant ΔK test the load is consistently decreased as the crack extends to hold ΔK constant, therefore if the crack length measurement from the dcPD system is off the final measured crack length the ΔK value is higher or lower than expected. This means that when posttest correction is applied the crack growth rate (da/dN) will be faster or slower over time depending on the crack length error. This error will not appear until posttest processing.

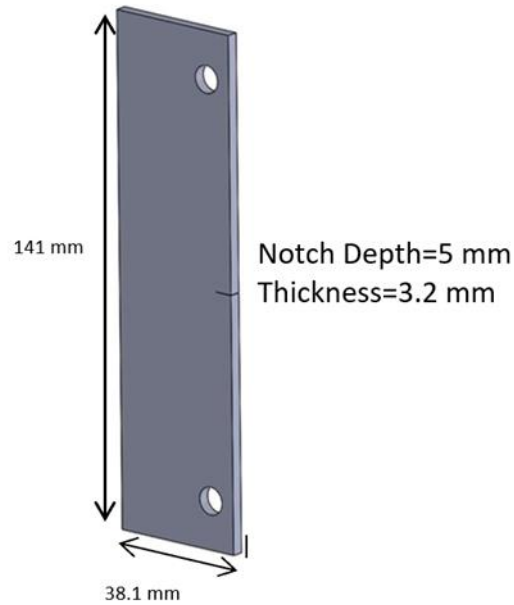


Figure 1
Eccentrically Loaded Single Edge Notch Tension (ESE(T)) sample. All dimensions are in millimeters (mm).

² FTA division of Laboratory Testing Inc 2331 Topaz Drive Hatfield, PA 19440

³ MTS Systems Corporation 14000 Technology Drive Eden Prairie, MN USA 55344

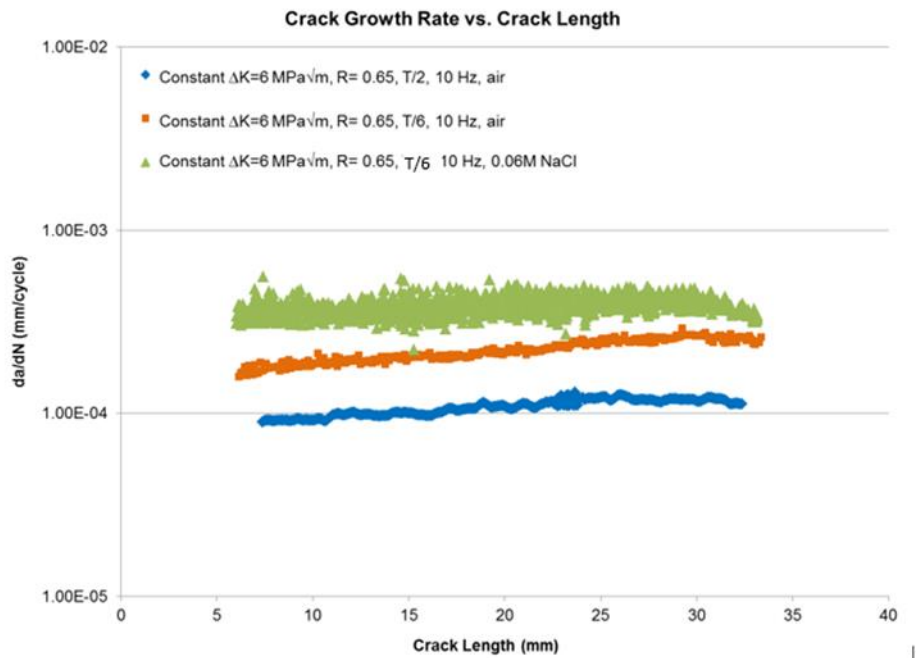


Figure 2
Constant ΔK , R testing for AA7075-T651 ESE(T) sample showing proper K-solution control.

Middle tension (M(T)) specimens per ASTM E647 were milled from 6.35 mm thick AA7075-T651 to final dimensions of 102 mm wide by 406 mm long as shown in Figure 1 [43]. Specimen length was oriented in the rolling (loading) direction and thicknesses ranged from 5 to 6 mm depending on the amount of material removal required for each individual specimen to meet the flatness requirements of the standard [43]. Electrical discharge machining was not used for any manufacturing during this program [44].

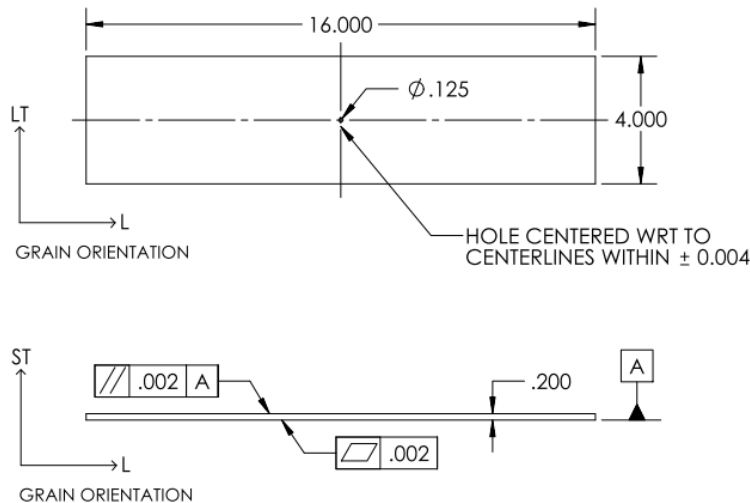


Figure 1
Excerpt of engineering drawing of 102 mm by 406 mm M(T) test specimen, drawing dimension in inches.

The starter notches were first milled as slots, then sharpened manually with a custom-manufactured cutting blade as described previously [45]. The gage section of the specimen around the starter notch was polished to enhance

resolution of the crack during surface optical crack length measurements. Fatigue crack growth rate (FCGR) tests were performed on a 250 kN capacity MTS Systems 810 servohydraulic mechanical test frame with the specimen gripped by the bolt and keyway clamps described in the M(T) specimen annex of ASTM E647 and shown in Figure 2 [43].



Figure 2
Bolt and keyway clamps gripping M(T) test specimen

Atmospheric Corrosion Effects on Fatigue Crack Growth

Environmental fatigue testing was completed with both single parameter relative humidity (RH) control and varying RH control to determine the effect of a simulated atmospheric salt film of sodium chloride (NaCl) on fatigue crack growth rates. For the constant RH tests, the RH was held static at 90% for corrosion fatigue testing of ESE(T) samples with $400 \mu\text{g}/\text{cm}^2$ NaCl applied to the samples surface [45, 46]. The environment was a salt film of approximately $400 \mu\text{g}/\text{cm}^2$ sodium chloride (NaCl) applied evenly to the surface by pipetting a known amount of salt solution on to the sample surface and flash evaporating the solution [45, 46]. The value of $400 \mu\text{g}/\text{cm}^2$ was used as accelerated coastal salt loading amount bases on published work on environmental contaminants [44]. The acceleration is about 10 times the highest coastal value. The thin ends of the sample were not salted. Care was also taken to not fill the sample notch with solution. The salt film was then controlled by relative humidity. Two ΔK values, 4 and $6 \text{ MPa}\sqrt{\text{m}}$, were evaluated along with two stress ratios (R), 0.1 and 0.65. The frequency (f) was 0.15 Hz. The test frequency was selected based on the frequencies being aircraft loading relevant while limiting test time [45, 47-51].

Testing was completed to determine the effect of wetting and drying on crack growth rates using the ESE(T) specimen with $400 \mu\text{g}/\text{cm}^2$ thin film NaCl applied. The applied salt film was then rehydrated and controlled using relative humidity during the fatigue testing [39]. The RH was varied between 30% and 90% using active an RH control system which held the RH within approximately 1% of the set value. Thirty percent RH was selected for the lower

value as NaCl should be dry under that RH and not causing corrosion to occur [52, 53]. Two ΔK values, 4 and 6 $\text{MPa}\sqrt{\text{m}}$, were evaluated along with two stress ratios, 0.1 and 0.65 mentioned previously. The frequency was held constant at 1 Hz. Tests were started in a 30% RH environment and the crack was grown for a minimum of 1mm. Once the 1mm of growth was achieved, the specimen surface was wetted by increasing the RH in the test cell to 90% and the crack was grown for an additional 1 mm. The final step was to dry the specimen by returning the test cell to 30% RH. This process was then be repeated for the next set of mechanical load parameters. The RH was allowed to change as fast as possible and typically stabilized within 5 minutes. The fatigue crack was allowing to continue propagating during these RH changes.

Complex atmospheric environmental fatigue tests were completed using the M(T) sample under combinations of ozone, relative humidity, salt film and temperature in an effort to determine how the combined environmental parameters effect fatigue crack growth. The salt film was applied and controlled with RH. Specimens were precracked at least 1 millimeter (mm) in laboratory air conditions at an R of 0.1 with a *K*-shedding protocol with the normalized *K*-gradient, *C*, equal to -0.08 mm^{-1} and a cyclic loading frequency (*f*) of 10 Hz. For the test phase, specimens were loaded under a constant cyclic amplitude, starting at or above a ΔK of 3 $\text{MPa}\sqrt{\text{m}}$, an *R* of 0.65, and a cyclic loading frequency of 10 Hz.

For the environmental application for both sample designs, previously developed environmental control systems are being used. This flow-through environmental control system is designed to maintain a constant flow of humidified air and ozone that is mixed prior to entering the test cell. Relative humidity is generally controlled to within $\pm 1\%$ and ozone to within ± 2 ppm passively. Each environmental parameter can be applied in combination or individually. Similarly, the gas lines can be connected to a variety of chambers. The temperature control uses a custom thermal chamber designed to work with a MTS servohydraulic load frame. These environmental control systems are described in other publications [45, 46].

RESULTS AND DISCUSSION

Figure 5 shows the crack length versus cycles for a sample tested at a single set of mechanical loading parameters, $\Delta K=6\text{MPa}\sqrt{\text{m}}$, $R=0.1$, $f=0.15$ Hz and a single set of environmental parameters, $400\mu\text{g}/\text{cm}^2$ NaCl salt loading held at 90% RH. The goal of this test was to verify that the hydrated salt environment is able to enter the crack evenly over the course of a long fatigue test, often in excess of 3 to 5 weeks. The test performed well and had a highly linear crack growth rate as evidenced by the linear fit until approximately 22mm of crack growth. At 22mm of crack length the crack suddenly arrested and after waiting over a week the crack never grew again. The reason for this crack arrest is unknown. However, the test did show that the environment was reaching the crack for very long crack lengths as the crack growth rate is near that of full immersion, which would also be expected for a 90% RH value [54, 55]. This result is in line with other published work examining fatigue crack growth rates of aluminum alloys under atmospheric conditions [49, 50, 58]. While accelerated crack growth rates above full immersion have been noted, the cause is typically attributed to a wetting and drying cycle during testing [55-57]. Adjustments to the RH will also change the film layer thickness which can also effect corrosion rates under atmospheric conditions [55-57].

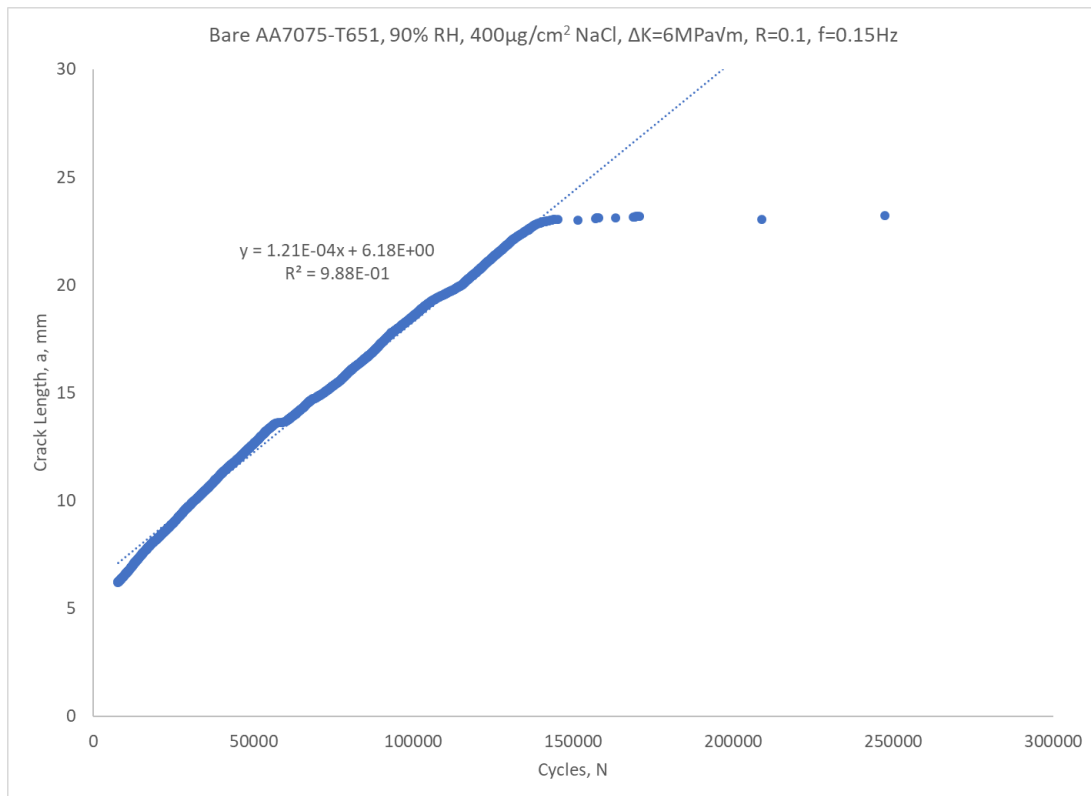


Figure 5
Crack length versus cycles (*a* versus *N*) plot for a sample tested at a single environmental parameter to verify environmental ingress. The slope of the line is the crack growth rate (da/dN).

Figure 6 shows the wetting and drying fatigue crack growth rate data taken for the sample with $400 \mu\text{g}/\text{cm}^2$ NaCl applied to the surface and then controlled by varying the RH between 30% and 90% (shaded regions Figure) to determine the effects of wetting and drying on atmospheric corrosion fatigue. If there was no lag between the hydration and ingress of the surface salt and the increase in FCGR, a square wave would be the expected shape of the response as the increase in RH happens over the course of approximately five minutes. The data shows some amount of lag time for changes in RH, however it was confirmed that the salt is affecting the crack growth rates once the RH changes, as the crack growth rates for all of the high humidity regions were close to full immersion NaCl conditions. When the sample was put through a drying cycle the data shows an increase in crack growth rates as the RH drops towards 30%, this increase in crack growth rate is likely actually occurring and supports drying cycle being the more aggressive environment [55-57]. The reason for this acceleration in crack growth during drying is theorized to be related to increased oxygen reduction with decreasing solution layer thickness or the critical chloride concentrations being achieved to allow for pitting to begin as the crack dries [55-57]. Either of which could increase anodic dissolution and the related cathodic reactions under the thin film condition which would increase hydrogen production which could lead to hydrogen embrittlement and increase the environmentally assisted fatigue crack growth rates during the drying cycle [55-57]. Similar crack propagation results have been noted by other researchers on 5xxx and 7xxx series aluminum alloys undergoing atmospheric wetting and drying tests under stress corrosion cracking conditions [55-57]. More recent publications support the increase in crack growth rate is likely due to the decreasing solution layer thickness as compared to the chloride concentration change [55].

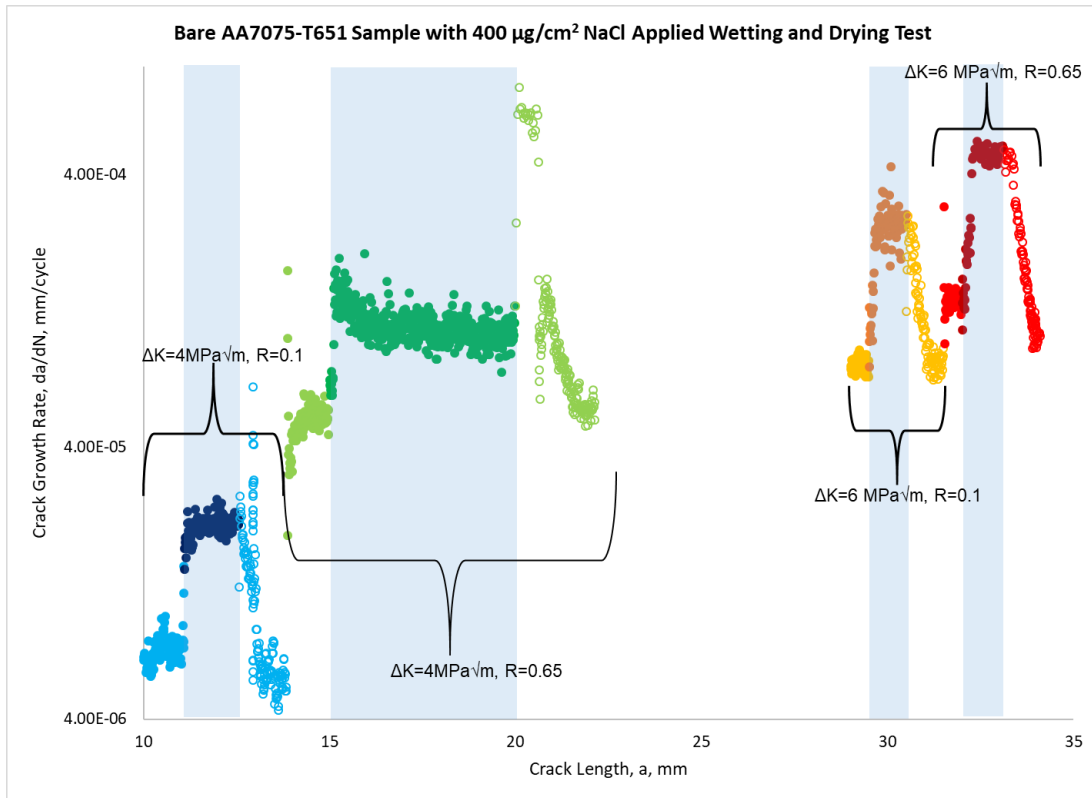


Figure 6

Effect of atmospheric wetting and drying on FCGRs for various constant ΔK , constant R mechanical loading conditions. The shading on the chart denotes the application of 90% RH for each loading condition, areas without shading were tested at 30% RH. The test frequency was 1 Hz for the entire test.

Complex Environmental Testing

Various combinations of environmental parameters have also been tested. The results of the ozone, salt film and RH have been documented in other publications [45, 46, 59]. Figure 7 shows the results of testing using the M(T) sample, under laboratory air baseline conditions (red triangles) compared to ozone at 30 ppm (gray squares), ozone (30 ppm) with 80% RH (green circles) and ozone (30 ppm) with 80% RH with a 400 $\mu\text{g}/\text{cm}^2$ NaCl film added to the surface of the sample (black x-marks), all testing was completed at a frequency of 10 Hz and a R of 0.65. The loading frequency of 10 Hz was selected to allow for each test to be finished in under a month; however this high frequency will limit environmental exposure at the crack tip.

The presence of ozone in dry air did not affect the crack growth rate of the alloy, this result was somewhat expected, due to the ozone not reacting with the crack tip to form an oxide capable of slowing crack growth rates. This is in line with other research published on silver where the presence of ozone without water vapor is insufficient to produce oxidizing effects due to the lack of atomic oxygen [39,40]. The loading frequency of 10 Hz also limits the time available for oxide formation, testing at a lower frequency could allow for oxides to form with dry ozone. When water vapor was added to the ozone, the crack growth rate drops to below the baseline data up to a ΔK of almost 8 $\text{MPa}\sqrt{\text{m}}$, then the crack growth rate increases over that of the dry baseline. The decrease in crack growth rate is from the combined effects of ozone with relative humidity allowing for an oxide film to develop on the crack tip protecting the crack from the moist environment, above a ΔK of 8 $\text{MPa}\sqrt{\text{m}}$, the ability of that oxide film to withstand the mechanical loading breaks down. When the salt film is added to the sample surface, the crack growth rates initially fall in line with the dry air baseline data, showing that the combined presence of the chloride with the increased oxide layer is only able to protect the crack growth rates down to a dry air condition. Between a ΔK of approximately 5.2 and 7 $\text{MPa}\sqrt{\text{m}}$, the crack growth rate is reduced to the levels noted during the wet test with ozone added, this shows that the chloride is not reaching the crack tip during this portion of the test, either due to oxide film development or other phenomenon, possibly sample drying. Once the crack exceeded ΔK of 7 $\text{MPa}\sqrt{\text{m}}$ the crack growth rate matches the 85% RH test with ozone added, showing that the mechanical driving force has taken over the crack growth rate. It should be noted that based on previously published work on silver and accelerated

corrosion damage, the inhibiting effects of ozone on the crack growth rates in aluminum were somewhat unexpected and need to be further explored [38, 39, 40, 60,61]. These results also highlight that corrosion accelerating oxidizers for some material systems may not produce the same results for other material systems based on oxides and corrosion products formed.

Post fatigue testing, the fracture surface was examined with a scanning electron microscope (SEM) and using energy dispersive x-ray spectroscopy (EDS) to confirm the presence of corrosion damage and chlorides on the sample surface. The EDS confirmed sodium chloride was present across the fatigue surface all the way to the crack tip just prior to the overload region.

For this program, temperature was added as a variable. First testing was completed at a temperature of -60°C, shown as black stars. Then testing was completed with salt film and ozone added with the -60°C temperature, blue triangles. The effect of ozone which in prior tests appeared to slow FCGR with RH and salt film has no effect at low temperature. These types of tests, are important because the results can help guide which environmental parameters are critical for accelerated laboratory test method development.

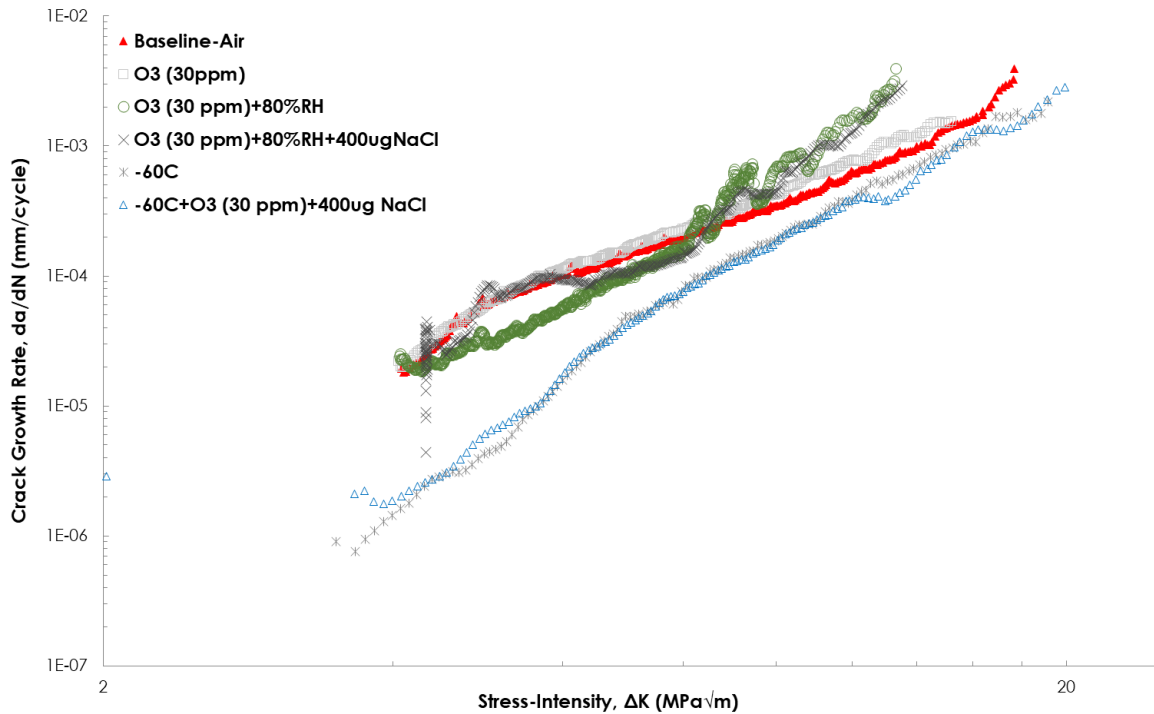


Figure 7
Effect of various complex environmental parameters on FCGR in 7075-T651.

Laboratory Comparison

One of the other goals of this program is to define the variability of complex environmental fatigue data produced in different laboratories. To begin that comparison first the baseline laboratory air crack growth rate data measured at Ohio State and SAFE were compared for the same lot of AA7085-T7451. Figure 8 shows the results of this comparison, which have excellent agreement.

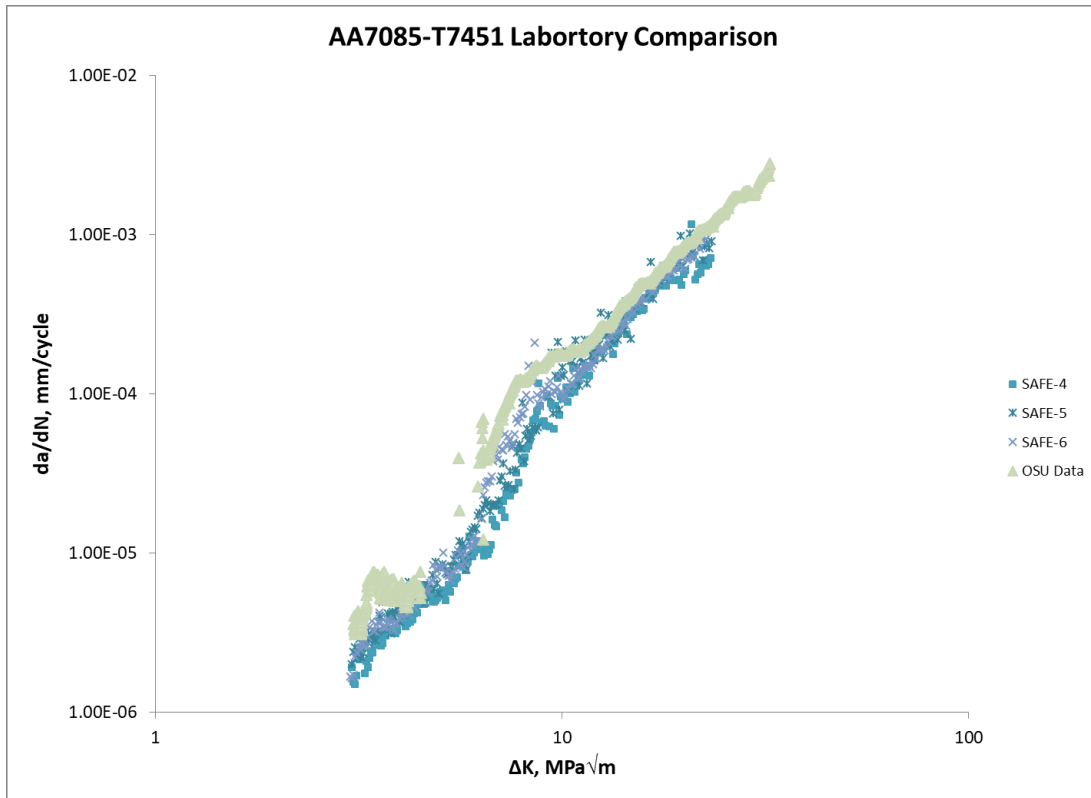


Figure 8
Comparison fatigue crack growth rate data for laboratory air tests taken at two locations for AA7085-T7451.

CONCLUSIONS

Fatigue testing with complex atmospheric environments on aluminum alloys has shown that producing consistent results that relate back to effects with individual parameters or results without load application is difficult. As such, the goal of this program is to provide insight into how these individual and combined environmental parameters effect fatigue crack growth in aerospace aluminum alloys. Another aim is for two separate laboratories to produce robust, repeatable results fatigue crack growth rate results under laboratory atmospheric environments. These combined results can then be used to determine which environmental parameters dominate allowing for improved laboratory testing methods for atmospheric corrosion of aluminum alloys. Currently it has been shown that the two laboratories have excellent agreement with fatigue crack growth rates in laboratory air tests. It has also been shown that ozone has limited effect of fatigue crack growth at -60C using a loading frequency of 10 Hz.

ACKNOWLEDGEMENTS

This work was funded under a USAFA Broad Agency Announcements (FA7000-14-2-0013, FA-7000-15-2-0012 and FA7000-18-2-0001) by the Office of Naval Research Science and Technology and by the United States Office of the Secretary of Defense Corrosion Policy and Oversight Office under the Technical Corrosion Collaboration (TCC). Some research was completed at the United States Air Force Academy Center for Aircraft Structural Life Extension (CASTLE).

The views and conclusions contained herein are those of the authors and should not be interpreted as necessarily representing the official policies and endorsements, either expressed or implied, of the US Air Force Academy or

the US Government. This material is declared a work of the United States Government and is not subject to copyright protection in the United States.

REFERENCES

1. Findlay, S. & Harrison, N. Why aircraft fail. *Materials today* 5, 18-25 (2002).
2. Shoales, G. A., Fawaz, S. A. & Walters, M. R. in *ICAF 2009, Bridging the Gap between Theory and Operational Practice* 187-207 (Springer, 2009).
3. Gangloff, R. P. in *Environment Induced Cracking of Metals* (eds R.P. Gangloff & M.B Ives) 55-109 (NACE, 1989).
4. Wei, R. P. & Gangloff, R. P. in *Fracture Mechanics: Perspectives and Directions, ASTM STP 1020* (eds R.P. Wei & R.P Gangloff) 233-264 (ASTM International, 1989).
5. Ford, F. & Andresen, P. L. *Corrosion in nuclear systems: environmentally assisted cracking in light water reactors. Corrosion Technology-New York and Basel-* 17, 605-642 (2002).
6. Ford, F. P. & Andresen, P. L. in *Advances in Fracture Research* (ed K. Salema) 1571-1584 (Pergamon Press, 1989).
7. Corsetti, L. & Duquette, D. The Effect of Mean Stress and Environment on Corrosion Fatigue Behavior of 7075-T6 Aluminum. *Metallurgical and Materials Transactions B* 5, 1087-1093 (1974).
8. Feeney, J. A., McMillan, J. C. & Wei, R. P. Environmental Fatigue Crack Propagation of Aluminum Alloys at Low Stress Intensity Levels. *Metallurgical Transactions* 1, 1741-1757 (1970).
9. Ford, F. P. Corrosion Fatigue Crack Propagation in Aluminum-7% Magnesium Alloy. *Corrosion* 35, 281-287 (1979).
10. Gingell, A. D. B. & King, J. E. The Effect of Frequency and Microstructure on Corrosion Fatigue Crack Propagation in High Strength Aluminium Alloys. *Acta Materialia* 45, 3855-3870 (1997).
11. Holroyd, N. J. H. & Hardie, D. Factors Controlling Crack Velocity in 7000 Series Aluminium Alloys During Fatigue in an Aggressive Environment. *Corrosion Science* 23, 527-531, 533-546 (1983).
12. Khobaib, M., Lynch, C. T. & Vahldiek, F. W. Inhibition of Corrosion Fatigue in High Strength Aluminum Alloys. *Corrosion* 37, 285-292 (1981).
13. Nakai, Y., Alavi, A. & Wei, R. Effects of Frequency and Temperature on Short Fatigue Crack Growth in Aqueous Environments. *Metallurgical and Materials Transactions A* 19, 543-548 (1988).
14. Piascik, R. S. & Gangloff, R. P. Environmental Fatigue of an Al-Li-Cu Alloy: Part I. Intrinsic Crack Propagation Kinetics in Hydrogenous Environments. *Metallurgical and Materials Transactions A* 22, 2415-2428 (1991).
15. Stoltz, R. E. & Pelloux, R. M. Inhibition of Corrosion Fatigue in 7075 Aluminum Alloys. *Corrosion* 29, 13-17 (1973).
16. Lynch, S. P. Mechanisms of Environmentally Assisted Cracking in Al-Zn-Mg Single Crystals. *Corrosion Science* 22, 925-937 (1982).
17. Wei, R. P. Fatigue-Crack Propagation in a High-Strength Aluminum Alloy. *International Journal of Fracture Mechanics* 4, 159-168 (1968).
18. Lee, E. U., Vasudevan, A. K. & Glinka, G. Environmental Effects on Low Cycle Fatigue of 2024-T351 and 7075-T651 Aluminum Alloys. *International Journal of Fatigue* 31, 1938-1942 (2009).
19. Piascik, R. S. & Gangloff, R. P. in *Environment Induced Cracking of Metals* (eds R.P. Gangloff & M.B. Ives) 233-239 (NACE, 1989).
20. Pao, P. S., Imam, M. A., Cooley, L. A. & Yoder, G. R. Comparison of Corrosion-Fatigue Cracking of Aluminum-Lithium Alloy AA 2090-T8E41 and Alloy AA 7075-T651 in Salt Water. *Corrosion* 45, 530-535 (1989).
21. Gasem, Z. & Gangloff, R. P. in *Chemistry and Electrochemistry of Corrosion and Stress Corrosion Cracking* (ed R.H. Jones) 501-521 (TMS-AIME, 2001).

22. Gasem, Z. M. Frequency Dependent Environmental Fatigue Crack Propagation in the 7XXX Alloy/Aqueous Chloride System Ph.D. thesis, University of Virginia, (1999).
23. Green, A. M. & Knott, J. F. in *Advances in Fracture Research* (ed K. Salama) 1747-1756 (Pergamon Press, 1989).
24. Warner, J. S. & Gangloff, R. P. Alloy induced inhibition of fatigue crack growth in age-hardenable Al–Cu Alloys. *International Journal of Fatigue* 42, 35-44, doi:10.1016/j.ijfatigue.2011.04.013 (2012).
25. Warner, J. S., Kim, S. & Gangloff, R. P. Molybdate Inhibition of Environmental Fatigue Crack Propagation in Al-Zn-Mg-Cu. *International Journal of Fatigue* 31, 1952-1965 (2009).
26. Lin, F. & Starke, E. A. in *Hydrogen Effects in Metals* (eds I.M. Bernstein & A.W Thompson) 485-492 (TMS-AIME, 1980).
27. Wanhill, R. Fractography of Fatigue Crack Propagation in 2024-T3 and 7075-T6 Aluminum Alloys in Air and Vacuum. *Metallurgical and Materials Transactions A* 6, 1587-1596 (1975).
28. Carter, R., Lee, E., Starke, E. & Beevers, C. The Effect of Microstructure and Environment on Fatigue Crack Closure of 7475 Aluminum Alloy. *Metallurgical and Materials Transactions A* 15, 555-563 (1984).
29. Gao, M., Wei, R. P. & Pao, P. Chemical and Metallurgical Aspects of Environmentally Assisted Fatigue Crack Growth in 7075-T651 Aluminum Alloy. *Metallurgical and Materials Transactions A* 19, 1739-1750 (1988).
30. Pao, P. S., Gao, M. & Wei, R. P. Environmentally Assisted Fatigue-Crack Growth in 7075 and 7050 Aluminum Alloys. *Scripta Metallurgica* 19, 265-270 (1985).
31. Ruiz, J. & Elices, M. Effect of Water Vapor Pressure and Frequency on Fatigue Behaviour in 7017-T651 Aluminium Alloy Plate. *Acta Materialia* 45, 281-293 (1997).
32. Hartman, A. On the Effect of Oxygen and Water Vapor on the Propagation of Fatigue Cracks in 2024-T3 Alclad Sheet. *International Journal of Fracture Mechanics* 1, 167-188 (1965).
33. Bradshaw, F. J. & Wheeler, C. The Effect of Environment on Fatigue-Crack Growth in Aluminum and some Aluminum Alloys. *Applied Materials Research* 5, 112-120 (1966).
34. Broom, T. & Nicholson, A. Atmospheric Corrosion Fatigue of Age Hardenable Aluminum Alloys. *Journal of the Institute of Metals* 89, 183-190 (1960-1961).
35. Schuetz, W. Corrosion fatigue- The forgotten factor in assessing durability. ICAF 95- Estimation, enhancement and control of aircraft fatigue performance, 1-51 (1995).
36. Finlayson-Pitts, B. J. & Pitts, J. N. *Chemistry of the Upper and Lower Atmosphere*. (Academic Press, 2000).
37. Leygraf, C. & Graedel, T. *Atmospheric Corrosion*. (Wiley-Interscience, John Wiley & Sons, 2000).
38. International, A. Vol. B117 (ASTM International, West Conshohocken, PA, 2003).
39. Chen, Z. et al. Influence of UV irradiation and ozone on atmospheric corrosion of bare silver. *Corrosion Engineering, Science and Technology* 45, 169-180 (2010).
40. Liang, D. et al. Effects of sodium chloride particles, ozone, UV, and relative humidity on atmospheric corrosion of silver. *Journal of the electrochemical society* 157, C146-C156 (2010).
41. Khullar, P. & Kelly, R. G. in *NACE Corrosion Conference*. (NACE).
42. Cole, I., Azmat, N., Kanta, A. & Venkatraman, M. What really controls the atmospheric corrosion of zinc? Effect of marine aerosols on atmospheric corrosion of zinc. *International materials reviews* 54, 117-133 (2009).
43. Vol. E647-08 671-715 (ASTM International. West Conchohocken, PA).
44. Saravanan R. Arunachalam, Sarah E. Galyon Dorman, Richard T. Buckley, N. Aidan Conrad, Scott A. Fawaz, "Effect of electrical discharge machining on corrosion and corrosion fatigue behavior of aluminum alloys" *International Journal of Fatigue*, June 2018, Vol 111, pp. 44-53.
45. S.E. Galyon Dorman, J. H. Niebuhr, S. R. Arunachalam, R. T. Buckley, and S. A. Fawaz. (2018). Predicting and Managing Atmospheric Corrosion in DOD High Strength Aluminum Alloys. SAFE Inc.

46. Niebuhr, J.H., Galyon Dorman, S.E., Arunachalam, S.R, Rausch, J.W. and Fawaz, S.A., (2019) "Effect of Simulated Accelerated Atmospheric Environment Conditions on Fatigue Crack Growth Rates," CORROSION <https://doi.org/10.5006/2974>.
47. S.E. Galyon Dorman, (2017) "The Effect of Corrosion Inhibitors on the Corrosion Fatigue of a Legacy Aluminum Alloy, " DoD and Allied Nations Corrosion Conference, 2017-471006 (Birmingham, AL, Oct, 1, 2017).
48. Sarah E. Galyon-Dorman, Saravanan Arunachalam, and Scott A. Fawaz (2017). Effect of Chromate on Corrosion Fatigue in Service Relevant Concentrations. The 29th Symposium of the International Committee on Aeronautical Fatigue, Nagoya, Japan.
49. J.S. Warner, (2010) "The Inhibition of Environmental Fatigue Crack Propagation in Age-Hardenable Aluminum Alloys." PhD Dissertation, University of Virginia, Charlottesville, VA.
50. J.S. Warner, S. Kim and R.P. Gangloff, (2009) International Journal of Fatigue vol. 31, p. 1952-1965
51. R.J.H.Wanhill (2002), "Flight Simulation Fatigue Crack Growth Guidelines," NLR-TP-2001-545.
52. E.Schindelholz, B.E. Risteen and R.G. Kelly, "Effect of Relative Humidity on Corrosion of Steel under Sea Salt Aerosol Proxies," J. Electrochem. Soc. 2014 volume 161, issue 10, C450-C459.
53. E Schindelholz, E. (2014). "Towards Understanding Surface Wetness and Corrosion Response of Mild Steel in Marine Atmospheres." PhD Dissertation, University of Virginia, Charlottesville, VA.
54. E. Schindelholz, R.G. Kelly, "Wetting phenomena and time of wetness in atmospheric corrosion: a review," CORROSION REVIEWS, 30, 5-6 (December 2012): pp.135-170.
55. James Dante, Erica Macha, & Marta Zuflacht (2017), "Development of an Accelerated Dynamic Corrosion Test Method," SERPD WP-1673 Final Report.
56. Fritz Friedersdorf, (2018) "The influence of dynamic atmospheric conditions on EAC and corrosion fatigue" Stress-Assisted Corrosion Damage V, July 15 - 20, 2018, Schloss Hernstein, Hernstein, Austria.
57. Brown, N., Kramer, P., Friedersdorf, F., Schindelholz, M. & Siegel, J. in DoD-Allied Nations Corrosion Conference. 1351-1362.
58. S.E. Galyon Dorman, et al, (2016) Managing Environmental Impacts of Time-Cycle Dependent Structural Integrity of High Performance DoD Alloys, SAFE Inc., SAFE-RTP-16-045.
59. Galyon Dorman, S.E., Rausch, J.W., Niebuhr, J.H., Arunachalam, S.R., Fawaz, S.A., (2018) "The Effect of Corrosion Inhibitors on Corrosion Fatigue under Complex Environmental Conditions," Proceedings of the 2018 NACE Corrosion Conference, Phoenix, AZ, April 2018.
60. J. Schijve,. Fatigue of structures and materials. 2. Dordrecht: Springer Netherlands, 2009. ISBN 0-7923-7013-9.
61. W. Schütz. Corrosion fatigue- The forgotten factor in assessing durability. ICAF 95- Estimation, enhancement and control of aircraft fatigue performance. 1995. P. 1–51.